UC Irvine
UC Irvine Previously Published Works

Title

Exenatide promotes cognitive enhancement and positive brain metabolic changes in PS1-KI mice but has no effects in 3xTg-AD animals

Permalink

https://escholarship.org/uc/item/4157h8w9

Journal

Cell Death and Disease, 4(5)

ISSN

2041-4889

Authors

Bomba, M
Ciavardelli, D
Silvestri, E
et al.

Publication Date

2013-05-01

DOI

10.1038/cddis.2013.139

Peer reviewed

npg

Exenatide promotes cognitive enhancement and positive brain metabolic changes in PS1-KI mice but has no effects in 3xTg-AD animals

M Bomba[1,2,8], D Ciavardelli[1,3,4,8], E Silvestri[5], LMT Canzoniero[5], R Lattanzio[4], P Chiappini[4], M Piantelli[4], C Di Ilio[4], A Consoli[6] and SL Sensi*[,1,2,7]

Recent studies have shown that type 2 diabetes mellitus (T2DM) is a risk factor for cognitive dysfunction or dementia. Insulin resistance is often associated with T2DM and can induce defective insulin signaling in the central nervous system as well as increase the risk of cognitive impairment in the elderly. Glucagone like peptide-1 (GLP-1) is an incretin hormone and, like GLP-1 analogs, stimulates insulin secretion and has been employed in the treatment of T2DM. GLP-1 and GLP-1 analogs also enhance synaptic plasticity and counteract cognitive deficits in mouse models of neuronal dysfunction and/or degeneration. In this study, we investigated the potential neuroprotective effects of long-term treatment with exenatide, a GLP-1 analog, in two animal models of neuronal dysfunction: the PS1-KI and 3xTg-AD mice. We found that exenatide promoted beneficial effects on short- and long-term memory performances in PS1-KI but not in 3xTg-AD animals. In PS1-KI mice, the drug increased brain lactate dehydrogenase activity leading to a net increase in lactate levels, while no effects were observed on mitochondrial respiration. On the contrary, exenatide had no effects on brain metabolism of 3xTg-AD mice. In summary, our data indicate that exenatide improves cognition in PS1-KI mice, an effect likely driven by increasing the brain anaerobic glycolysis rate.

Type 2 diabetes mellitus (T2DM) is characterized by impaired glucose homeostasis and insulin resistance in peripheral tissues. Deregulation of glucose metabolism and insulin signaling impair memory and learning in animal models of diabetes as well as in elderly T2DM patients.[1] Interestingly, previous studies have suggested that some pathogenic mechanisms of Alzheimer's disease (AD) significantly overlap with those present in T2DM,[2] thereby suggesting commonalities between the two pathological conditions.

As examples of the commonalities between the two pathologies, recent studies indicate that T2DM, like AD, produces a variety of neurochemical, neuroanatomical, and behavioral changes that can be linked to acceleration of brain aging,[3] increased oxidative stress,[4,5] and neuroendocrine alterations.[6] Animal models of diabetes exhibit atrophy of dendrites of hippocampal pyramidal neurons, decreased spine density, increased neuronal vulnerability, and decreased neurogenesis,[7,8] all common features of AD and AD animal models. Interestingly, insulin therapy inhibits or reverses most of these neurological changes,[9,10]

thereby supporting the assumption that the hormone has an important role in modulating neurotrophic and neuroendocrine functions.

Glucagon like peptide-1 (GLP-1) is an incretin hormone[11] that controls insulin and glucose homeostasis.[12] Binding of GLP-1 to its receptor (GLP-1R) is coupled with multiple signal transduction pathways that lead to the activation of adenylyl cyclase, protein kinase c (PKC) and mitogen activated protein (MAP) kinase.[13] GLP-1R agonists act on β-cells to stimulate insulin secretion and increase glucose-dependent insulin release. These drugs are therefore successfully employed for T2DM treatment.

In addition to its role in glycaemic control, GLP-1 has neuroprotective properties. GLP-1 acts as growth factor in the brain, induces neurite outgrowth and protects against oxidative injury in cultured neurons.[14] GLP-1Rs are expressed on human neurons throughout the brain[15] and on large pyramidal neurons in the cortex and hippocampus of mice.[14] Mice overexpressing hippocampal GLP-1Rs show increased neurite growth and improved learning.[16]

Exenatide, a GLP-1 receptor agonist with longer half-life than the native molecule, is widely used in the treatment of T2DM. Interestingly, exenatide induces neuronal progenitor cell proliferation in mouse brains.[16] Moreover, in animal studies, the drug has been shown to enhance synaptic plasticity and cognitive performance.[17]

For these reasons, exenatide has been proposed as a therapeutic agent in neurological conditions like Parkinson's disease (PD) and Alzheimer's disease (AD).[17,18]

In this study, we investigated the effects of long-term (9 month) intraperitoneal (IP) administration of exenatide on memory performance, brain mitochondrial function, and anaerobic glycolysis in two models of neuronal dysfunction: the presenilin-1 knock-in (PS1-KI) mice and the triple transgenic mouse model of AD (3xTg-AD).

PS1-KI mice overexpress mutant (M146V) presenilin-1, a mutation leading to increased amyloid peptides (Aβ) production and linked to the development of familial AD (FAD). Given the amino-acidic sequence of murine Aβ (that is not prone to metal-dependent aggregation),[19] PSI-KI mice do not develop Aβ-dependent pathology nor show intra-extraneuronal deposits of amyloid.[20] However, previous studies have shown that PS1-KI mice exhibit signs of neural and brain dysfunction. This genotype develops impaired spatial learning and memory deficits in an age-dependent fashion.[21] PS1-KI hippocampal neurons also display increased vulnerability to excitotoxicity as well as deregulation of intracellular Ca^{2+}.[22] Thus, these mice represent a model of amyloid-independent neuronal dysfunction.

In the study, we have also investigated exenatide effects on 3xTg-AD mice. 3xTg-AD mice harbor human mutant PS1 (PS1$_{M146V}$) along with human mutant APP (APP$_{swe}$) and tau (tau $_{P301L}$) protein.[23] This model displays the major pathological features of the AD brain and develops early signs of synaptic dysfunction that proceed in parallel with the age-dependent appearance of Aβ and tau pathology.[20]

Results

Exenatide does not alter body weight in PS1-KI and 3xTg-AD mice. Previous studies in exenatide-treated mice or rats have shown that the hypoglycaemic action of the drug is associated with reduction of food intake and decreased gain in weight.[24] In order to verify whether the drug has the same effects in our animal models, we investigated changes in body weight of treated and untreated PS1-KI and 3xTg-AD mice. No statistically significant effects were found in the two genotypes ($P = 0.285$). It should be noted that 7-month-old 3xTg-AD mice gained statistically significant more weight compared with PS1-KI mice, a phenomenon that is independent of drug treatment as indicated by three-factor ANOVA showing significant effect of genotype (Figure 1; $P = 2 \times 10^{-9}$). Percentage values of body-weight gain occurring in animals between 5–7 months of age (m.o.a.) were $10 \pm 2\%$ for PS1-KI or $25 \pm 3\%$ for 3xTg-AD mice.

Exenatide improves short- and long-term memory in PS1-KI mice but has no effects on 3xTg-AD animals. PS1-KI mice undergo progressive impairment of spatial
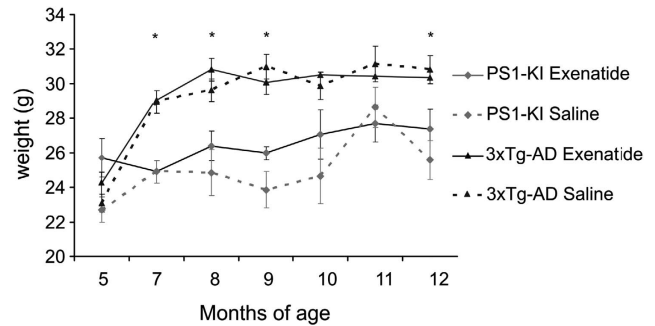

Figure 1 Exenatide effects on body weight of PS1-KI and 3xTg-AD mice. Graphs depict time-course of body weight changes monitored in treated and untreated PS1-KI and 3xTg-AD mice. Untreated genotypes showed a physiological time-dependent gain in weight. 3xTg-AD mice gained significantly more weight ($P < 0.050$) compared with PS1-KI animals when growing from 5–7 month of age. Exenatide treatment did not affect body weigh in both genotypes. Data are presented as mean values $\pm$ the standard error of the mean (S.E.M.). '*' indicates significant differences ($P < 0.050$) between the two genotypes

learning and memory at 9–11 m.o.a.,[21] while 3xTg-AD mice show age-dependent spatial memory decline developing as early as 5–6 m.o.a.[23]

With the Morris water maze (MWM), a task that measures hippocampus-dependent spatial memory,[25] we tested effects of exenatide treatment on memory performances of the two mouse models.

In PSI-KI mice at 6 m.o.a., three-factor ANOVA followed by *post-hoc* multiple comparisons indicated significant ($P = 0.048$) effects of treatment on escape latency evaluated 1.5 h after the end of the last training trial, an index of short-term memory performance (Figure 2a).

The same statistical analysis revealed enhanced long-term memory in treated PS1-KI mice at 6 m.o.a. (Figure 2b; $P = 0.026$). In the study group, out of the untreated mice, four were male and three female; in the treated PSI-KI mice, three were male and two female, no gender-related effects were observed.

In the 3xTg-AD mice, no signs of learning deficits were present in the 4-day training sessions (data not shown). Three-factor ANOVA showed significant effects of genotype on MWM parameters, such as target quadrant occupancy (T target) recorded 1.5 h and 24 h after the end of last training trial ($P = 2 \times 10^{-5}$ and $P = 7 \times 10^{-5}$, respectively), time spent in the opposite quadrant (T opposite; $P = 2 \times 10^{-2}$) and number of platform location crosses ($P = 2 \times 10^{-3}$) recorded 1.5 h after the end of last training trial. Untreated 3xTg-AD mice at 12 m.o.a showed decreased number of platform crosses 1.5 h after the end of the last training. (Figures 2c and d), thereby indicating impaired spatial memory compared with PS1-KI mice. Furthermore, 6-month-old 3xTg-AD mice, 1.5 h and 24 h after the end of the last training, spent significantly more time in the opposite quadrants (Figures 2g and h) than in the target quadrant (Figures 2e and f) independently of the treatment, further suggesting the presence of initial cognitive deficits in 3xTg-AD mice.

Analysis of the same MWM parameters in treated 3xTg-AD mice revealed no beneficial effects of the exenatide treatment.
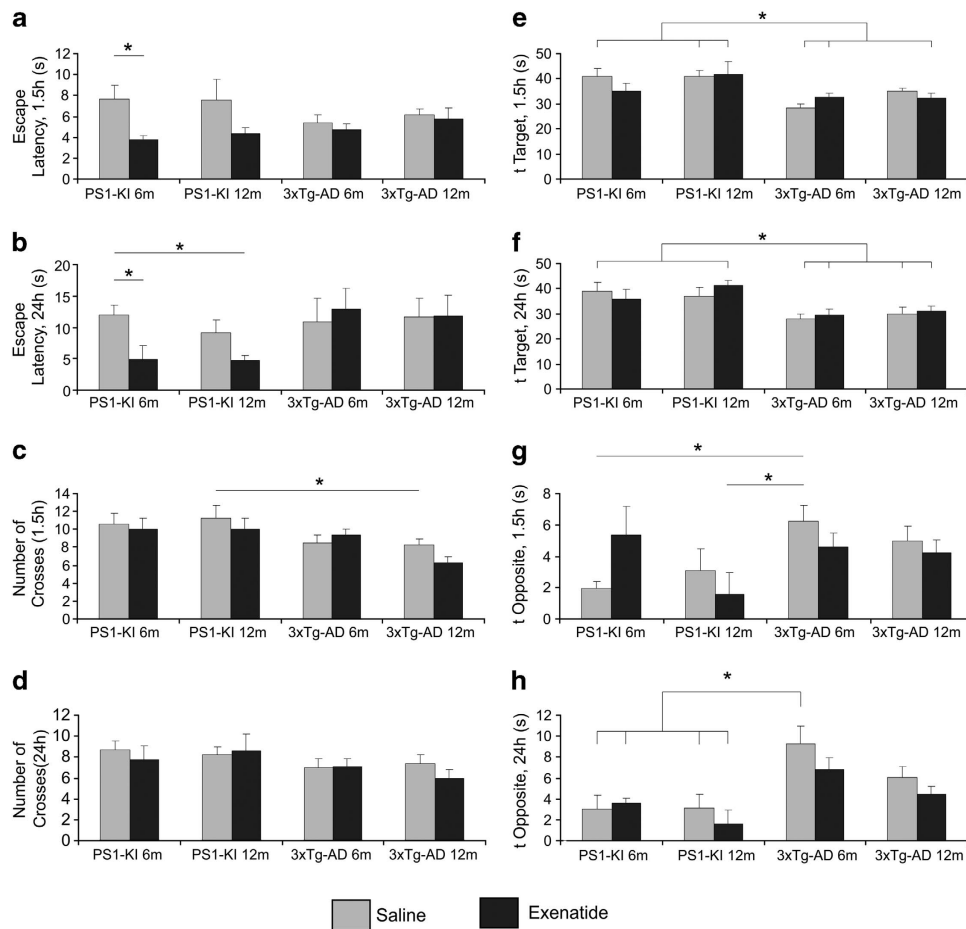
Figure 2 Effects of exenatide on short- and long-term memory in PS1-KI and 3xTg-AD mice. Memory performances were evaluated with the MWM test. Bar graphs depict: (a) Short-term memory performance, as assessed with time latencies of MWM, performed 1.5 h after the last training session, in treated and untreated 6- and 12 m.o.a. PS1-KI and 3xTg-AD mice. Analysis reveals statistically significant decrease in latency values compared with age-matched untreated mice (*$P = 0.048$) only for the 6 m.o.a. PS1-KI animals. No positive effects were seen in 6- and 12 m.o.a. 3xTg-AD mice. (b) Long-term memory performance, as assessed with time latencies of MWM, performed 24 h after the last training session, in treated and untreated PS1-KI and 3xTg-AD mice. Analysis of 6 m.o.a. exenatide-treated mice showed statistically significant decrease in latency values compared with age-matched untreated mice (*$P = 0.026$) only in PS1-KI animals. No positive effects were seen in 3xTg-AD mice. (c) Short-term memory and (d) long-term memory performances, as assessed with platform crosses of MWM, performed 1.5 h or 24 h, after the last training session, in treated and untreated 6 and 12 m.o. PS1-KI and 3xTg-AD mice. Analysis showed statistically significant decrease in the number of platform crosses at 1.5 h in untreated 12 m.o.a. 3xTg-AD compared with age-matched untreated PS1-KI mice (*$P = 0.002$). (e) Short-term memory and (f) long-term memory performances, as assessed with T target of MWM, performed at 1.5 h and 24 h, in treated and untreated PS1-KI and 3xTg-AD mice. Analysis showed statistically significant decrease in time spent in the T target at 1.5 h ($P = 0.00002$) and 24 h ($P = 0.00007$) in untreated and treated 6- and 12 m.o.a. 3xTg-AD mice compared with age-matched treated and untreated PS1-KI mice. (g) Short-term memory and (h) long-term memory performances, as assessed with T opposite of MWM, performed at 1.5 h and 24 h, in treated and untreated PS1-KI and 3xTg-AD mice. Analysis showed statistically significant increase in time spent in the T opposite 1.5 h and 24 h in untreated 6 m.o. 3xTg-AD mice ($P = 0.020$) compared with treated and untreated PS1-KI mice at 6 and 12 m.o.a. Data are presented as mean values ± the standard error of the mean (S.E.M.). '*' indicates $P < 0.050$

Exenatide does not counteract age-dependent development of Aβ and tau pathology in 3xTg-AD mice. Given the lack of beneficial cognitive effects on treated 3xTg-AD mice, we evaluated whether the drug had changed Aβ and/or tau pathology in these animals.

Previous studies have shown that *in vitro* treatment with GLP-1 or GLP-1 analogs (including exenatide) reduce brain levels of Aβ and amyloid precursor protein (APP) in cultured neurons.[26] We did not find significant reductions of intraneuronal Aβ levels (Figure 3e; $P = 0.552$) in the hippocampus of treated 3xTg-AD mice.

As previously reported, our 3xTg-AD mice at 12 m.o.a. showed extensive hippocampal h-tau immunoreactivity in the CA1 subfield. In accordance with other studies,[26] exenatide

treatment did not decrease h-tau immunoreactivity in 3xTg-AD mice (Figure 3f; $P = 0.337$).

Exenatide does not affect brain mitochondrial COX activity in PSI-KI and 3xTg-AD mice. GLP-1 and GLP-1 analogs possess anti-apoptotic and neuroprotective properties. In that respect, these molecules have also been reported to reduce neuronal injury triggered by oxidative stress.[15,27] Impairment of mitochondrial functioning along with increased reactive oxygen species (ROS) production have been shown in brains of PS1-KI[28,29] and 3xTg-AD mice.[30,31]

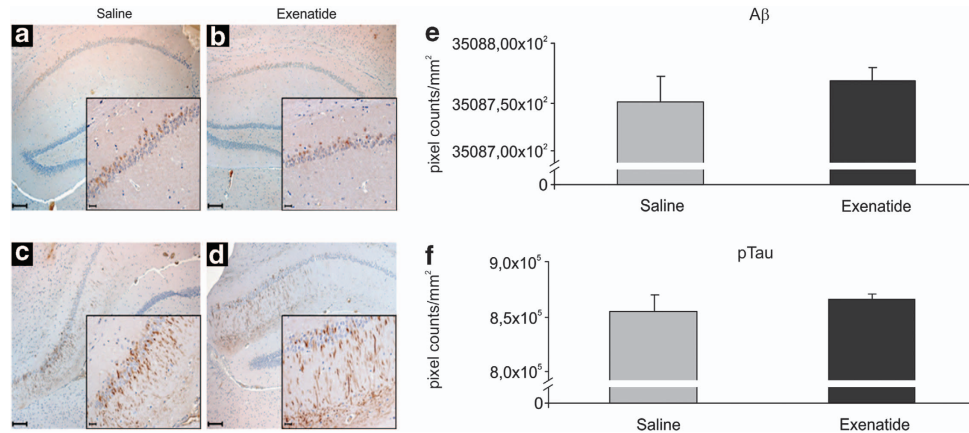To evaluate effects of exenatide treatment on mitochondrial respiration, we measured COX activity in mitochondria

Figure 3 Exenatide does not reduce Aβ and tau pathology in 3xTg-AD mice. Immunohistochemistry was employed to detect deposits of intraneuronal Aβ (**a and b**) and h-tau (**c and d**) in brain slices from treated ($n = 5$) and untreated ($n = 5$) 3xTg-AD mice. Low magnification (20 ×; scale bar = 100 μM) images of intraneuronal Aβ deposits in untreated (**a**) or treated (**b**) 3xTg-AD mice. Insets show a high magnification (40 ×) view of hippocampal CA1 areas (scale bar = 20 μM). No differences are seen between treated and untreated mice as shown by quantification of intraneuronal Aβ loads (**e**). Low magnification (20 ×) images of h-tau deposits in untreated (**c**) or treated (**d**) 3xTg-AD mice. Insets show a high magnification (40 ×) view of hippocampal CA1 areas (scale bar = 20 μM). No differences are seen between treated and untreated mice as shown by quantification of h-tau levels (**f**). Quantification of intraneuronal Aβ or h-tau levels is expressed with bar graphs of mean pixel counts for mm^2 ± the standard deviation (S.D.)

obtained from PS1-KI or 3xTg-AD brains. No significant effects upon treatment were found.

Significant effects were observed when analyzing differences in the two genotypes with increased COX activity in 3xTg-AD mice compared with PS1-KI animals (Figure 4a: $P = 0.001$).

Exenatide increases brain forward LDH activity in PS1-KI mice but has no effect in 3xTg-AD animals. To gain further insight into the effects of exenatide on brain glucose metabolism and anaerobic glycolysis in particular, we assayed forward (LDH$_{Pyr \rightarrow Lac}$) and reverse (LDH$_{Lac \rightarrow Pyr}$) LDH activities in cytosolic fractions of brain samples collected from treated and untreated PS1-KI or 3xTg-AD mice.

Two-factor ANOVA showed significant main effect of genotype ($P = 0.002$) and significant interaction between genotype and treatment ($P = 0.032$), thereby indicating differences between the mouse strains in LDH$_{Pyr \rightarrow Lac}$ activity in response to treatment. We observed higher LDH$_{Pyr \rightarrow Lac}$ activity in treated PS1-KI mice compared with untreated and treated 3xTg-AD mice (treated PS1-KI versus untreated 3xTg-AD, $P = 0.014$; treated PS1-KI versus treated 3xTg-AD, $P = 0.001$) and found that exenatide significantly increased (by 34%) LDH$_{Pyr \rightarrow Lac}$ in PS1-KI mice (Figure 4b; $P = 0.048$,), while no effects were observed in 3xTg-AD animals. Two-factor ANOVA indicated no statistical significance for LDH$_{Lac \rightarrow Pyr}$ activity in treated PS1-KI mice compared with untreated or treated 3xTg-AD mice (Figure 4c).

Exenatide enhances anaerobic glucose catabolism in brains of PS1-KI mice. Targeted metabolomic analysis of glycolytic, Krebs cycle intermediates, and related amino acids was performed by gas-chromatography mass spectrometry (GC–MS) to verify whether exenatide had produced a metabolic shift to anaerobic glycolysis in treated mice. PSI-KI

mice showed increased levels of brain lactic acid compared with 3xTg-AD mice independently from drug treatment (Figure 5; Supplementary Table 1). No differences between the genotypes were observed for Krebs cycle intermediates and related amino acids with the exception of increased fumaric acid and reduced glutamic acid in PS1-KI mice (Supplementary Table 1).

Interestingly, exenatide treatment produced marked increases of β-hydroxybutyric acid and lactic acid in PS1-KI mice (Figure 5, Supplementary Table 1). Furthermore, in PSI-KI mice, exenatide promoted a trend effect toward increased brain levels of glucose and glycolytic intermediates such as glucose 6-phosphate (G-6P, $P = 0.206$) and 3-phosphoglyceric acid (3-PG, $P = 0.116$) (Figure 5; Supplementary Table 1). No significant changes were observed in treated 3xTg-AD mice (Supplementary Table 1).

Discussion

GLP-1 has an important role in brain insulin signaling and glucose homeostasis and its receptor is highly expressed through the brain. Exenatide, the synthetic agonist of the GLP-1 receptor, has neurotrophic and neuroprotective properties in vitro.[32] Mechanisms underlying these properties are still not completely understood.

In this study, we sought to determine whether exenatide has beneficial effects on cognitive performances in two models of brain dysfunction: the PS1-KI$_{M146V}$ mouse, a model that shows cognitive decline developed in an Aβ-independent way and the 3xTg-AD mouse, an animal that display an Aβ-and tau-dependent AD-like cognitive and neurodegenerative phenotype.

We found that the drug promoted positive effects on short- and long-term memory in PS1-KI mice, while no benefits were produced in 3xTg-AD mice.

It should be noted that our 12-month-old PS1-KI mice did not show signs of age-related cognitive decline, thereby
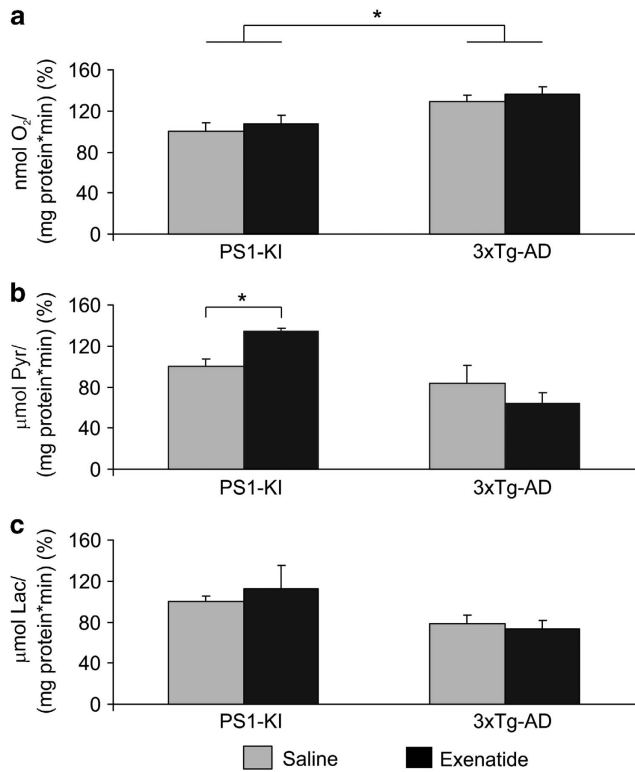
Figure 4 Effects of exenatide on brain COX and LDH in PS1-KI and 3xTg-AD mice. (a) Bar graphs show mitochondrial COX activity in 12-month-old treated and untreated PS1-KI and 3xTg-AD mice. Exenatide had no effects on the mitochondrial respiration of PS1-KI and 3xTg-AD mice. Of note, treated and untreated 3xTg-AD mice showed significantly increased COX activity when compared with PS1-KI mice (untreated PS1-KI *versus* untreated 3xTg-AD mice, $P = 0.014$; untreated PS1-KI *versus* treated 3xTg-AD mice, $P = 0.003$; treated PS1-KI *versus* untreated 3xTg-AD mice, $P = 0.062$; treated PS1-KI *versus* treated 3xTg-AD mice, $P = 0.017$). COX activity is expressed as $nmol_{O2}/mg_{prot}/min$ normalized for brain protein concentration. Data are shown as percentage of mitochondrial COX activity found in untreated PS1-KI mice and presented as mean values $\pm$ the standard error of the mean (S.E.M.). (b) Forward and (c) reverse brain LDH activities in 12-month-old treated and untreated PS1-KI and 3xTg-AD mice. Exenatide treatment induced significant increase of forward LDH activity in PS1-KI mice ($P = 0.048$). Of note, treated PS1-KI mice showed higher forward LDH activity compared to untreated ($P = 0.014$) and treated ($P = 0.001$) 3xTg-AD mice. LDH activity is expressed as $\mu mol_{Substrate}/mg_{Protein}/min$ normalized for brain protein concentration. Data are shown as percentage of brain LDH activities found in untreated PS1-KI mice and presented as mean values $\pm$ (S.E.M.). '*' indicates $P < 0.050$

Figure 5 Effects of exenatide on brain concentrations of glucose, glycolytic intermediates, and lactic acid in PS1-KI and 3xTg-AD mice. Bar graphs on the right show brain concentrations of glycolytic intermediates as listed in the left metabolic flow chart (glucose; glucose 6-phosphate (G-6P); glyceraldehyde 3-phosphate (GA3P); 3-phosphoglyceric acid (3-PG), and lactic acid). Exenatide significantly increased lactic acid concentrations in brains of PS1-KI mice ($P = 0.033$). Of note, increased brain levels of lactic acid are also found in untreated PS1-KI mice compared with untreated ($P = 0.002$) and treated ($P = 0.010$) 3xTg-AD mice as well as treated PS1-KI mice compared with the same study groups ($P = 0.010$ and 0.008, respectively). Furthermore, exenatide significantly increased brain concentration glucose ($P = 0.018$ and 0.009), G-6P ($P = 0.010$ and 0.008), and GA3P ($P = 0.062$ and 0.007) in treated PS1-KI mice compared with untreated and treated 3xTg-AD mice, respectively. Concentrations are expressed as ng/mg (wet weight). Bars show mean values $\pm$ the standard error of the mean (S.E.M.). '*' indicates $P < 0.050$

suggesting that exenatide may act as cognitive enhancer on mice that still have a valid cognitive reserve. Our results are in line with previous studies in non-transgenic rodents.[33]

Exenatide had no effect on memory performances of 3xTg-AD mice. No frank signs of learning deficits were observed in our 12-month-old 3xTg-AD animals. However, changes indicative of initial memory deficits appeared when analyzing several MWM parameters. 3xTg-AD mice showed statistically significant worse short- and long-term performances as evaluated with t-target and t-opposite indices (Figures 2e–h); they also showed impaired number of crosses when evaluating short-term memory (Figures 2c and d). Thus, it can be assumed that the cognitive reserve of these mice is already compromised. This idea goes along with the observed
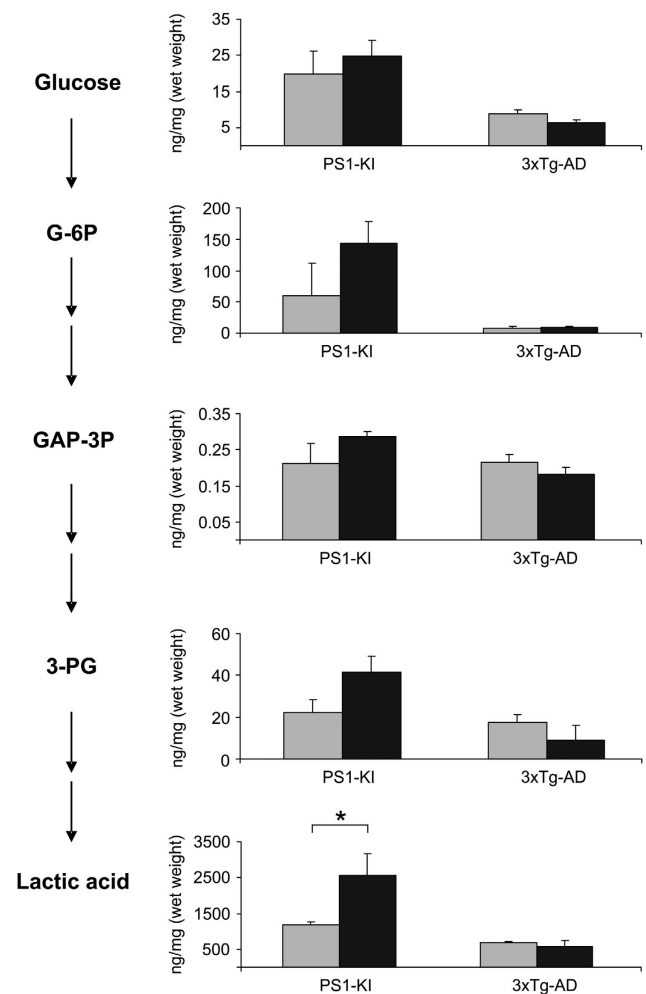
significant intraneuronal accumulation of Aβ and h-tau, two pathological hallmarks that were unaffected by the exenatide treatment.

Our findings are not in line with a recent study showing that the drug is effective in counteracting AD-like cognitive decline and pathology in another AD transgenic mouse model (APPSwe/PS1ΔE9).[34] The discrepancy between the two studies may be related to differences in pathology of the employed strains (our model expresses both Aβ- and tau-dependent pathology, while the other study made use of Tg

animals showing only Aβ-driven pathology) and to the length of treatment (9 months in our case, while the other study administered the drug twice a day for 3 weeks in animals at 13–14 m.o.a.).

Exenatide has also been shown to counteract cognitive deficits present in 3xTg-AD mice that were made insulin-resistant by administration of streptozotocin. However, in accordance with our results, the same study showed that in control 3xTg-AD mice (i.e., not treated with streptozotocin) exenatide failed to reduce Aβ pathology.[26] Our findings are in agreement with previous data also indicating that exenatide does not reduce Aβ accumulation in brains of another Tg AD model.[35]

Previous reports have indicated an anorexant effect of exenatide on rodents.[24] We did not observe significant changes in age-related weight gain in both mouse strains after treatment. This finding is not completely surprising because the anorexant effect of exenatide has been mostly reported in mouse models of T2DM or obesity, while it has not observed in healthy rodents.

It should be noted that our PS1-KI mice showed less age-dependent gain in weight compared with 3xTg-AD mice. These data are in line with a previous study for our group in which we evaluated effects of pioglitazone treatment in PS1-KI, 3xTg-AD, and WT mice.[36] In the study, we showed different metabolic features between PSI-KI and 3xTg-AD mice that may indicate differences in metabolism and, ultimately, in brain energetics.

In that regard, we have also previously showed that compared with PS1-KI mice, 3xTg-AD animals exhibit decreased mitochondrial complex I and IV activities in the cortex and hippocampus.[37,38] Furthermore, we have recently reported that compared with PS1-KI mice, 3xTg-AD animals also show decreased expression levels of brain LDH, the key enzyme of anaerobic glycolysis.[39]

Overall, these data suggest that the cognitive improvement found for PS1-KI mice may reflect the effects of exenatide on the brain metabolism of these animals, a process that seems less compromised compared with 3xTg-AD mice.

Mitochondria are an important source of ROS, molecules that are critical modulators of the synaptic pathology associated with aging and neurodegenerative disease.[26,27,40–42]

GLP-1 and GLP-1 analogs as well as their endogenous proteolytic by-products can prevent mitochondrial deficits, increase mitochondrial ATP synthesis and counteract brain oxidative stress especially by decreasing the production of mitochondrial ROS. Thus, we evaluated whole-brain COX activity as a marker of mitochondrial function in both mouse strains. No significant changes of COX activity were observed in PS1-KI or 3xTg-AD mice after treatment but, surprisingly, PS1-KI animals showed decreased activity when compared with 3xTg-AD mice. These findings are not in line with our previous data indicating that, compared with 3xTg-AD, PS1-KI mice show increased activity of mitochondrial complex IV in the hippocampus and cortex.[37,38] In that respect, it is important to point out that in contrast to the previous study, the present data are obtained from whole-brain samples and not from homogenates of specific brain areas.[37,38] This experimental difference is important as COX

activity in AD brains show modifications of opposite direction depending on the specific subregional localization of the enzyme.[43] Furthermore, enhanced COX activity and mitochondrial oxygen consumption may, of course, imply increased generation of ATP, but also enhanced production of injurious ROS.

In our study, exenatide treatment had no effects on COX activity, thereby suggesting that, in PSI-KI mice, the beneficial cognitive effects of the drug are likely not linked to an increase in mitochondrial oxygen consumption. One potential caveat to this explanation is related to the fact that, as mentioned above, analysis was performed on whole-brain samples, thereby leaving open the possibility that subregional differences in activity may be present. Another potential limitation arises from the fact that while the observed unchanged COX activity indirectly supports the hypothesis that exenatide is not affecting ROS production, our study has not directly addressed this point by evaluating multiple ROS species, like hydrogen peroxide and lipid peroxides.

In search for mechanisms, we also investigated the effects of exenatide on an additional energetic pathway such as the anaerobic glycolysis and studied brain LDH activities. We found increased $LDH_{Pyr \to Lac}$ activity in treated PS1-KI mice (Figure 4b). This finding suggests that exenatide can promote a metabolic shift toward anaerobic glycolysis in this genotype. Targeted metabolomic analysis further substantiated this idea by revealing enhanced glycolytic rate and higher brain lactate levels in treated PS1-KI mice, an effect that was not observed in 3xTg-AD mice.

Increased lactate production has profound implication for cognition and can provide a valid conceptual framework for the cognitive enhancing effect of exenatide.

Lactate is the end-product of glycolysis and can be converted back to pyruvate in a reversible reaction catalyzed by LDH. This reaction provides significant energy source for the brain as intracerebral glycogen stores are relatively limited and, in the absence of exogenous glucose, rapidly consumed within few minutes.[44] In addition, neuronal gluconeogenic activity is negligible,[45] and thus, neurons largely depend on lactate as main energy substrate.[46,47]

Astrocytes are also important as they metabolize glucose and produce lactate that is exported to neighboring neurons through the activation of an astrocyte–neuron lactate shuttle.[48]

Lactate is not just an energy substrate. Recent data strongly indicate that the molecule promotes neuroprotection,[49] affects cognition, synaptic plasticity, and long-term potentiation (LTP).[50] In a landmark paper, Suzuki et al.[50] have demonstrated that lactate is indeed instrumental to promote LTP, thereby providing a mechanism for the beneficial cognitive effects deriving from the exenatide-dependent increases in lactate levels that we found in the PS1-KI mice. Thus, the positive cognitive effects observed in exenatide-treated PS1-KI mice can be, at least partially, explained by the increased brain levels of lactate produced by the drug.

Furthermore, supporting the idea of other beneficial mechanisms set in motion by exenatide, recent studies indicate that anaerobic glycolysis is neuroprotective[51] and that increased LDH expression and activity confer resistance to amyloid and other toxins by decreasing mitochondrial

respiration and ROS production.[52] In that respect, the drug may have produced positive cognitive effects by promoting an overall better survival of subsets of neurons that are strategic for cognition. Further studies are needed to clarify whether the drug is also able to directly counteract injurious processes like ROS production and oxidative stress.

Conclusions

Overall our findings indicate that exenatide has significant cognitive enhancing effects even when in presence, as for PS1-KI mice, of a genetic background that leads to neuronal dysfunction. It should be underlined that in our PSI-KI mice, we have not investigated $A\beta$ deposition as murine amyloid (although known to be increased in the genotype) shows an amino-acidic composition that does not favor aggregation and therefore plaque-dependent pathology cannot be expected. Thus, the beneficial activity of exenatide is likely targeting changes exerted by murine amyloid, a set of pathophysiological phenomena that do not require aggregation and plaque formation.

The favorable activities of exenatide probably rely on the induction of a metabolic switch toward anaerobic glycolysis as well as increased production of lactate, two phenomena that can fuel the neurons of brains in which a valid cognitive reserve is still present. In addition, this metabolic shift may also serve a neuroprotective role by counteracting oxidative stress in the brain. The sample size of the PS1-KI group is relatively small and the findings should be interpreted as positive and encouraging indication for further studies on a larger cohort of these animals. Moreover, our results also warrant further investigation in wild-type animals to assess whether exenatide can act as cognitive enhancer upon physiological conditions and/or brain aging. Finally, we would also like to stress that part of the novelty of the present paper arises from the fact that in a large cohort of 3xTg-AD mice, we failed to observe the beneficial effects of exenatide. Albeit negative, the finding is relevant as the 3xTg-AD animals show both amyloid and tau-dependent pathology and positive effects of exenatide have been so far proved only in amyloid-dependent Tg-AD models. Thus, these results raise the possibility that the drug may be not so effective in pathological scenarios, like the one offered by the 3xTg-AD, that more closely mimic the human disease.

Materials and Methods

Animals and treatment paradigm. Procedures involving animals and their care were approved by the institutional Ethics Committee (protocol no. AD-301) and conducted in conformity with institutional guidelines that are in compliance with national (DLn 116, GU, suppl 40, 18 February 1992) and international laws and policies. All efforts were made to minimize the number of animals used and their suffering. Thirty five 3xTg-AD animals (15 female and 20 male) and twelve PS1-KI animals (7 male and 5 female) were enrolled at 3 m.o.a. and randomly assigned for 9 months to exenatide or saline administration. Animals received daily IP injection of exenatide (500 μg/kg BW) or vehicle, 5 days a week. Body weight of treated and untreated mice was evaluated every month.

Morris water maze. The MWM apparatus consists of a circular plastic tank (1.3 m diameter) filled with water. The maze is located in a room containing several intra- and extra-maze visual cues. A visible platform was employed at the beginning of the MWM test to make sure that animals had no vision deficits. Mice were then trained to swim in the tank and climb on a (12 × 13 cm) rectangular

platform submerged (2 cm) beneath the water surface. Mice were given four trials per day for 4 consecutive days. To reduce the stress related to the task, mice were placed on the platform 10 s before the beginning of the first training session. Mice failing to find the platform within 90 s were manually guided to it and allowed to remain there for 10 s. Between trials, mice were placed back into a holding cage under a warming fan for 20 min. Retention of the spatial memory task was assessed 1.5 and 24 h after the end of the last training trial. Both probe trials consisted of a 60 s free swim in the pool without platform. Performances were evaluated in terms of time spent to reach and cross the platform location (escape latency), number of crosses over the platform location, time spent in target (T target) or opposite (T opposite) quadrants.

Tissues preparation and reagents. At the end of the treatment, mice were killed by carbon dioxide inhalation and tissue samples were collected. Brain were rapidly taken after removal of cerebellum and sagittally halved into two hemispheres. Samples were immediately frozen by liquid nitrogen and kept at $-80\,°C$ for subsequent analysis.

All chemicals and reagents were purchased from Sigma-Aldrich (Shnelldorf, Germany) unless otherwise specified.

Immunohistochemistry. Carnoy-fixed and paraffin-embedded brains of 3XTg-AD mice ($n = 5$ per group) were sagittally sectioned at 5 μm. Tissue sections were stained using anti-human phospho-Tau (thr-231) (1:100 dilution, overnight, clone AT180, Thermo Fisher Scientific, Rockford, IL, USA) and anti-human beta-amyloid (1:200 dilution, overnight, clone DE2B4, Abcam, Cambridge, UK). Antigen retrieval was performed in 10 mmol/l sodium citrate buffer (pH 6.0) by microwave treatment at 750 W for 10 min for phospho-Tau and by thermostatic bath at 100 °C for 10 min for beta-amyloid. The anti-mouse EnVision kit (Dako, Glostrup, Denmark) was used for signal amplification. In control sections, the specific primary antibody was omitted or replaced with isotype-matched immunoglobulins. Number of phospho-Tau or beta-amyloid stained pyramidal neurons was measured using Photoshop version 8.0 (Adobe System Incorporated, San Jose, CA, USA), as previously reported.[38]

Cytochrome oxidase activity. Cytochrome c oxidase (COX) activity was determined with polarography at 25 °C using a Clark oxygen electrode (Rank Brothers, Cambridge, England[53] and 1.5 ml of reaction medium containing 30 μM cytochrome c, 4 μM rotenone, 0.5 mM dinitrophenol, 10 mM sodium malonate, and 75 mM of 4-(2-hydroxyethyl)-1-piperazineethanesulfonic acid (Hepes) buffer (pH 7.4). Whole-brain samples were finely minced, diluted 1:10 (w/v) and homogenized in a modified Chappel–Perry medium containing 1 mM of adenosine 5′-triphosphate (ATP), 50 mM Hepes buffer adjusted to pH 7.4, 100 mM KCl, 5 mM MgCl$_2$, 1 mM of ethylenediamine N, N, N′, N′-tetraacetic acid (EDTA), and 5 mM of ethylene glycol tetraacetic acid (EGTA). Homogenates were then diluted 1:2 (v/v) in the same medium with polyethylene glycol ether W-1 (100 mg/g $_{tissue}$) in order to unmask tissue enzyme activity. Homogenates were then kept on ice for 30 min. COX activity was measured as differences between rates of oxygen consumption observed in homogenates after addition of substrate (4 mM sodium ascorbate with 0.3 mM N, N, N′, N′-tetramethyl-p-phenylenediamine) and rates of oxygen consumption observed in substrate alone (in order to take in account auto-oxidation of ascorbate). Results were reported as nmol$_{O_2}$/mg$_{prot}$/min.

Analysis of cytosolic LDH activities. Lactate dehydrogenase (LDH) direct (pyruvate (Pyr) to lactate (Lac) (LDH$_{Pyr\rightarrow Lac}$)) as well as reverse (Lac to Pyr (LDH$_{Lac\rightarrow Pyr}$)) activities were spectrometrically assayed as previously described[54] using a tunable microplate reader (Spectra max 190, Molecular Devices, Sunnyvale, CA, USA). Briefly, brain tissues were homogenized in phosphate buffer solution (PBS, 20 ml/g of tissue, 0.010 M, pH = 7.4). Homogenates were centrifuged at 2000 × g for 3 minutes at 4 °C to remove cell debris and nuclear pellets. Supernatants were further centrifuged 8000 × g for 10 minutes at 4°C in order to obtain cytosolic fractions. Protein concentration was determined according to the Bradford assay.[55] To measure LDH$_{Pyr\rightarrow Lac}$ activity, Pyr (25 μl, 2.50 g/l) and reduced nicotinamide adenine dinucleotide (NADH, 100 μl, 0.3 g/l) were added to the samples (50 μl). The decrease of absorbance at 340 nm was measured at 25 °C in 1-min intervals for 5 min. To measure LDH$_{Lac\rightarrow Pyr}$ activity, Lac (25 μl, 8.6 g/l) and oxidized nicotinamide adenine dinucleotide (NAD$^+$, 100 μl, 3.5 g/l) were added to samples (50 μl) after adjustment of pH to 8.8 with 0.05 M sodium pyrophosphate and increase of absorbance at 340 nm measured. LDH$_{Pyr\rightarrow Lac}$ and LDH$_{Lac\rightarrow Pyr}$ activities are expressed as μmol/mg$_{Protein}$/min.

GC–MS analysis of brain tissue. Gas-chromatography mass spectrometry (GC–MS) analysis of brain tissues collected from untreated and treated PS1-KI and 3xTg-AD mice ($n = 3$ for each study group) was performed as previously described.[56] Briefly, cytosolic brain homogenates (50 μl) were precipitated in cold 0.1% (v/v) methanolic trichloroacetic acid immediately after homogenization. Internal standards ($^{13}C_4$ malic acid, $^{13}C_4$ succinic acid, $^{13}C_6$ glucose; IS) were then added to give a final concentration of 10 μg/ml. Samples were centrifuged at $10000 \times g$ for 30 min and supernatants were collected and dried in a Speed Vac (Thermo Scientific, Milano, Italy). The dried extracts were derivatized with 20 μl of 20 mg/ml of methoxyamine hydrochloride solution in pyridine for 60 min at 70 °C, followed by reaction with 20 μl of N, O-bis(trimethylsilyl)trifluoroacetamide with 1% of trimethylchlorosilane for 60 min at 70 °C. GC–MS analysis was performed using a 6890N gas-chromatograph equipped with a 7863 Series auto-sampler and coupled with a 5973N mass spectrometer (Agilent Technologies, Palo Alto, CA, USA) operating in electron impact ionization mode. Three microliters were injected in pulsed-splitless mode by applying a pressure of 80 p.s.i. The injector temperature was kept at 250 °C. Chromatographic separations were obtained using a fused silica capillary column HP-5MS (30 m $\times$ 0.25 mm, Agilent Technologies). Helium was used as carrier gas at a constant flow rate of 1 ml/min. The GC oven was programed as follows: start at 70 °C (hold time, 1 min), which was raised at 4 °C/min to 300 °C (hold time, 5 min). The mass spectrometer was automatically calibrated using per-fluoro tributylamine as calibration standard. For quantification, the mass spectrometer was used in the selective ion monitoring mode and mass spectra were recorded in positive modes by monitoring the follow ions: m/z 147 (lactic acid; IS: $^{13}C_4$ succinic acid, m/z 251), m/z 191 (β-hydroxybutyric acid; IS: $^{13}C_4$ succinate, m/z 251), m/z 248 (glycine; IS: $^{13}C_4$ succinate, m/z 251), m/z 247 (succinic acid;; IS: $^{13}C_4$ succinate, m/z 251), m/z 245 (fumaric acid; IS: $^{13}C_4$ malic acid, m/z 236), m/z 320 (glutamic acid; IS: $^{13}C_4$ malic acid, m/z 236), m/z 233 (malic acid; IS: $^{13}C_4$ malic acid, m/z 236), m/z 218 (aspartic acid; IS: $^{13}C_4$ succinate, m/z 251), m/z 304 (γ-aminobutyric acid; IS: $^{13}C_4$ malic acid, m/z 236), m/z 328 (glyceraldheyde 3-phosphate; IS: $^{13}C_4$ malic acid, m/z 236), m/z 357 (3-phosphoglyceric acid; IS: $^{13}C_4$ malic acid, m/z 236), m/z 375 (citric acid; IS: $^{13}C_4$ malic acid, m/z 236), m/z 319 (glucose; IS: $^{13}C_6$ glucose, m/z 323), m/z 387 (glucose 6-phosphate; IS: $^{13}C_6$ glucose, m/z 323). Mass spectrometer parameters were: interface temperature 300 °C, ion source 250 °C, and quadrupole 150 °C. The external standard method and internal standard correction were applied for quantification of target metabolites. Data acquisition was performed using the G1701CA ChemStation software (Agilent Technologies).

Statistical analysis. Three-factor ANOVA and Fisher's least significant difference (LSD) post-hoc test were performed. Data were ranked and aligned taking in account their dependence. Aligned rank transformation (ART) of data was performed using the ART web software available at http://faculty.washington.edu/aimgroup/proj/art/artweb/. Genotype, treatment, and age were investigated. Unpaired two-tailed t-test was performed to assess statistical significance of differences in brain metabolite concentrations. Statistical tests were performed with a 95% confidence level. Statistical analysis was performed using Statistica 6.0 (Statsoft, Tulsa, OK, USA) software.

Conflict of Interest

The authors declare no conflict of interest.

1. Messier C, Gagnon M. Glucose regulation and cognitive functions: relation to Alzheimer's disease and diabetes. *Behav Brain Res* 1996; **75**: 1–11.
2. Talbot K, Wang HY, Kazi H, Han LY, Bakshi KP, Stucky A et al. Demonstrated brain insulin resistance in Alzheimer's disease patients is associated with IGF-1 resistance, IRS-1 dysregulation, and cognitive decline. *J Clin Invest* 2012; **122**: 1316–1338.
3. Magarinos AM, McEwen BS. Experimental diabetes in rats causes hippocampal dendritic and synaptic reorganization and increased glucocorticoid reactivity to stress. *Proc Natl Acad Sci USA* 2000; **97**: 11056–11061.

4. Grillo CA, Piroli GG, Rosell DR, Hoskin EK, McEwen BS, Reagan LP. Region specific increases in oxidative stress and superoxide dismutase in the hippocampus of diabetic rats subjected to stress. *Neuroscience* 2003; **121**: 133–140.
5. Reagan LP. Glucose, stress, and hippocampal neuronal vulnerability. *Int Rev Neurobiol* 2002; **51**: 289–324.
6. Leedom LJ, Meehan WP, Zeidler A. Avoidance responding in mice with diabetes mellitus. *Physiol Behav* 1987; **40**: 447–451.
7. Alvarez EO, Beauquis J, Revsin Y, Banzan AM, Roig P, De Nicola AF et al. Cognitive dysfunction and hippocampal changes in experimental type 1 diabetes. *Behav Brain Res* 2009; **198**: 224–230.
8. Kim YB, Kotani K, Ciaraldi TP, Henry RR, Kahn BB. Insulin-stimulated protein kinase C lambda/zeta activity is reduced in skeletal muscle of humans with obesity and type 2 diabetes: reversal with weight reduction. *Diabetes* 2003; **52**: 1935–1942.
9. Cheng B, Mattson MP. IGF-I and IGF-II protect cultured hippocampal and septal neurons against calcium-mediated hypoglycemic damage. *J Neurosci* 1992; **12**: 1558–1566.
10. Dore S, Kar S, Quirion R. Insulin-like growth factor I protects and rescues hippocampal neurons against beta-amyloid- and human amylin-induced toxicity. *Proc Natl Acad Sci USA* 1997; **94**: 4772–4777.
11. Kim SJ, Nian C, McIntosh CH. Glucose-dependent insulinotropic polypeptide and glucagon-like peptide-1 modulate beta-cell chromatin structure. *J Biol Chem* 2009; **284**: 12896–12904.
12. Lovshin JA, Drucker DJ. Incretin-based therapies for type 2 diabetes mellitus. *Nat Rev Endocrinol* 2009; **5**: 262–269.
13. Drucker DJ, Philippe J, Mojsov S, Chick WL, Habener JF. Glucagon-like peptide I stimulates insulin gene expression and increases cyclic AMP levels in a rat islet cell line. *Proc Natl Acad Sci USA* 1987; **84**: 3434–3438.
14. Hamilton A, Holscher C. Receptors for the incretin glucagon-like peptide-1 are expressed on neurons in the central nervous system. *Neuroreport* 2009; **20**: 1161–1166.
15. Perry T, Greig NH. Enhancing central nervous system endogenous GLP-1 receptor pathways for intervention in Alzheimer's disease. *Curr Alzheimer Res* 2005; **2**: 377–385.
16. During MJ, Cao L, Zuzga DS, Francis JS, Fitzsimons HL, Jiao X et al. Glucagon-like peptide-1 receptor is involved in learning and neuroprotection. *Nat Med* 2003; **9**: 1173–1179.
17. Perry TA, Greig NH. A new Alzheimer's disease interventive strategy: GLP-1. *Curr Drug Targets* 2004; **5**: 565–571.
18. Aviles-Olmos I, Limousin P, Lees A, Foltynie T. Parkinson's disease, insulin resistance and novel agents of neuroprotection. *Brain* 2013; **136**(Pt 2): 374–384.
19. Chen YR, Huang HB, Chyan CL, Shiao MS, Lin TH, Chen YC. The effect of Abeta conformation on the metal affinity and aggregation mechanism studied by circular dichroism spectroscopy. *J Biochem* 2006; **139**: 733–740.
20. Billings LM, Oddo S, Green KN, McGaugh JL, LaFerla FM. Intraneuronal Abeta causes the onset of early Alzheimer's disease-related cognitive deficits in transgenic mice. *Neuron* 2005; **45**: 675–688.
21. Sun X, Beglopoulos V, Mattson MP, Shen J. Hippocampal spatial memory impairments caused by the familial Alzheimer's disease-linked presenilin 1 M146V mutation. *Neurodegener Dis* 2005; **2**: 6–15.
22. Smith IF, Green KN, LaFerla FM. Calcium dysregulation in Alzheimer's disease: recent advances gained from genetically modified animals. *Cell Calcium* 2005; **38**: 427–437.
23. Oddo S, Caccamo A, Shepherd JD, Murphy MP, Golde TE, Kayed R et al. Triple-transgenic model of Alzheimer's disease with plaques and tangles: intracellular Abeta and synaptic dysfunction. *Neuron* 2003; **39**: 409–421.
24. Mack CM, Moore CX, Jodka CM, Bhavsar S, Wilson JK, Hoyt JA et al. Antiobesity action of peripheral exenatide (exendin-4) in rodents: effects on food intake, body weight, metabolic status and side-effect measures. *Int J Obes (Lond)* 2006; **30**: 1332–1340.
25. Sutherland RJ, McDonald RJ. Hippocampus, amygdala, and memory deficits in rats. *Behav Brain Res* 1990; **37**: 57–79.
26. Li Y, Duffy KB, Ottinger MA, Ray B, Bailey JA, Holloway HW et al. GLP-1 receptor stimulation reduces amyloid-beta peptide accumulation and cytotoxicity in cellular and animal models of Alzheimer's disease. *J Alzheimers Dis* **19**: 1205–1219.
27. Perry T, Holloway HW, Weerasuriya A, Mouton PR, Duffy K, Mattison JA et al. Evidence of GLP-1-mediated neuroprotection in an animal model of pyridoxine-induced peripheral sensory neuropathy. *Exp Neurol* 2007; **203**: 293–301.
28. Guo Q, Fu W, Sopher BL, Miller MW, Ware CB, Martin GM et al. Increased vulnerability of hippocampal neurons to excitotoxic necrosis in presenilin-1 mutant knock-in mice. *Nat Med* 1999; **5**: 101–106.
29. Trushina E, Nemutlu E, Zhang S, Christensen T, Camp J, Mesa J et al. Defects in mitochondrial dynamics and metabolomic signatures of evolving energetic stress in mouse models of familial Alzheimer's disease. *PLoS One* **7**: e32737.
30. Crouch PJ, Cimdins K, Duce JA, Bush AI, Trounce IA. Mitochondria in aging and Alzheimer's disease. *Rejuvenation Res* 2007; **10**: 349–357.
31. Yao J, Irwin RW, Zhao L, Nilsen J, Hamilton RT, Brinton RD. Mitochondrial bioenergetic deficit precedes Alzheimer's pathology in female mouse model of Alzheimer's disease. *Proc Natl Acad Sci USA* 2009; **106**: 14670–14675.
32. Perry T, Greig NH. The glucagon-like peptides: a new genre in therapeutic targets for intervention in Alzheimer's disease. *J Alzheimers Dis* 2002; **4**: 487–496.

33. Isacson R, Nielsen E, Dannaeus K, Bertilsson G, Patrone C, Zachrisson O et al. The glucagon-like peptide 1 receptor agonist exendin-4 improves reference memory performance and decreases immobility in the forced swim test. Eur J Pharmacol 650: 249–255.

34. Bomfim TR, Forny-Germano L, Sathler LB, Brito-Moreira J, Houzel JC, Decker H et al. An anti-diabetes agent protects the mouse brain from defective insulin signaling caused by Alzheimer's disease- associated Abeta oligomers. J Clin Invest 122: 1339–1353.

35. D'Amico M, Di Filippo C, Marfella R, Abbatecola AM, Ferraraccio F, Rossi F et al. Long-term inhibition of dipeptidyl peptidase-4 in Alzheimer's prone mice. Exp Gerontol 45: 202–207.

36. Masciopinto F, Di Pietro N, Corona C, Bomba M, Pipino C, Curcio M et al. Effects of long-term treatment with pioglitazone on cognition and glucose metabolism of PS1-KI, 3xTg-AD, and wild-type mice. Cell Death Dis 2013; 3: e448.

37. Corona C, Masciopinto F, Silvestri E, Viscovo AD, Lattanzio R, Sorda RL et al. Dietary zinc supplementation of 3xTg-AD mice increases BDNF levels and prevents cognitive deficits as well as mitochondrial dysfunction. Cell Death Dis 2010; 1: e91.

38. Corona C, Frazzini V, Silvestri E, Lattanzio R, La Sorda R, Piantelli M et al. Effects of dietary supplementation of carnosine on mitochondrial dysfunction, amyloid pathology, and cognitive deficits in 3xTg-AD mice. PLoS One 2011; 6: e17971.

39. Ciavardelli D, Silvestri E, Del Viscovo A, Bomba M, De Gregorio D, Moreno M et al. Alterations of brain and cerebellar proteomes linked to Abeta and tau pathology in a female triple-transgenic murine model of Alzheimer's disease. Cell Death Dis 2010; 1: e90.

40. Perry T, Greig NH. The glucagon-like peptides: a double-edged therapeutic sword? Trends Pharmacol Sci 2003; 24: 377–383.

41. Ma TC, Langley B, Ko B, Wei N, Gazaryan IG, Zareen N et al. A screen for inducers of p21(waf1/cip1) identifies HIF prolyl hydroxylase inhibitors as neuroprotective agents with antitumor properties. Neurobiol Dis 2012; 49C: 13–21.

42. Beal MF. Mitochondria take center stage in aging and neurodegeneration. Ann Neurol 2005; 58: 495–505.

43. Strazielle C, Jazi R, Verdier Y, Qian S, Lalonde R. Regional brain metabolism with cytochrome c oxidase histochemistry in a PS1/A246E mouse model of autosomal dominant Alzheimer's disease: correlations with behavior and oxidative stress. Neurochem Int 2009; 55: 806–814.

44. Brown AM, Ransom BR. Astrocyte glycogen and brain energy metabolism. Glia 2007; 55: 1263–1271.

45. Nelson T, Lucignani G, Atlas S, Crane AM, Dienel GA, Sokoloff L. Reexamination of glucose-6-phosphatase activity in the brain in vivo: no evidence for a futile cycle. Science 1985; 229: 60–62.

46. Bouzier-Sore AK, Voisin P, Canioni P, Magistretti PJ, Pellerin L. Lactate is a preferential oxidative energy substrate over glucose for neurons in culture. J Cereb Blood Flow Metab 2003; 23: 1298–1306.

47. Itoh Y, Esaki T, Shimoji K, Cook M, Law MJ, Kaufman E et al. Dichloroacetate effects on glucose and lactate oxidation by neurons and astroglia in vitro and on glucose utilization by brain in vivo. Proc Natl Acad Sci USA 2003; 100: 4879–4884.

48. Pellerin L, Pellegri G, Bittar PG, Charnay Y, Bouras C, Martin JL et al. Evidence supporting the existence of an activity-dependent astrocyte-neuron lactate shuttle. Dev Neurosci 1998; 20: 291–299.

49. Gordon GR, Choi HB, Rungta RL, Ellis-Davies GC, MacVicar BA. Brain metabolism dictates the polarity of astrocyte control over arterioles. Nature 2008; 456: 745–749.

50. Suzuki A, Stern SA, Bozdagi O, Huntley GW, Walker RH, Magistretti PJ et al. Astrocyte-neuron lactate transport is required for long-term memory formation. Cell 2011; 144: 810–823.

51. Newington JT, Pitts A, Chien A, Arseneault R, Schubert D, Cumming RC. Amyloid beta resistance in nerve cell lines is mediated by the Warburg effect. PLoS One 2011; 6: e19191.

52. Newington JT, Rappon T, Albers S, Wong DY, Rylett RJ, Cumming RC. Overexpression of pyruvate dehydrogenase kinase 1 and lactate dehydrogenase A in nerve cells confers resistance to amyloid beta and other toxins by decreasing mitochondrial respiration and reactive oxygen species production. J Biol Chem 2012; 287: 37245–37258.

53. Lanni A, Moreno M, Lombardi A, Goglia F. Calorigenic effect of diiodothyronines in the rat. J Physiol 1996; 494(Pt 3): 831–837.

54. Krieg AF, Rosenblum LJ, Henry JB. Lactate dehydrogenase isoenzymes a comparison of pyruvate-to-lactate and lactate-to-pyruvate assays. Clin Chem 1967; 13: 196–203.

55. Bradford MM. A rapid and sensitive method for the quantitation of microgram quantities of protein utilizing the principle of protein-dye binding. Anal Biochem 1976; 72: 248–254.

56. Kanani H, Chrysanthopoulos PK, Klapa MI. Standardizing GC–MS metabolomics. J Chromatogr B Analyt Technol Biomed Life Sci 2008; 871: 191–201.

Supplementary Information accompanies this paper on Cell Death and Disease website (http://www.nature.com/cddis)